Reaction pathways by quantum Monte Carlo: Insight on the torsion barrier of 1,3-butadiene, and the conrotatory ring opening of cyclobutene

Matteo Barborini and Leonardo Guidoni

Citation: J. Chem. Phys. **137**, 224309 (2012); doi: 10.1063/1.4769791
View online: http://dx.doi.org/10.1063/1.4769791
View Table of Contents: http://jcp.aip.org/resource/1/JCPSA6/v137/i22
Published by the American Institute of Physics.

Reaction pathways by quantum Monte Carlo: Insight on the torsion barrier of 1,3-butadiene, and the conrotatory ring opening of cyclobutene

Matteo Barborini[1,2] and Leonardo Guidoni[1]
[1]*Dipartimento di Matematica Pura ed Applicata, Università degli studi dell'Aquila, via Vetoio (Coppito 2), 67100 L'Aquila, Italy*
[2]*Dipartimento di Scienze Fisiche e Chimiche, Università degli studi dell'Aquila, via Vetoio (Coppito 2), 67100 L'Aquila, Italy*

(Received 5 October 2012; accepted 19 November 2012; published online 13 December 2012)

Quantum Monte Carlo (QMC) methods are used to investigate the intramolecular reaction pathways of 1,3-butadiene. The ground state geometries of the three conformers *s-trans*, *s-cis*, and *gauche*, as well as the cyclobutene structure are fully optimised at the variational Monte Carlo (VMC) level, obtaining an excellent agreement with the experimental results and other quantum chemistry high level calculations. Transition state geometries are also estimated at the VMC level for the *s-trans* to *gauche* torsion barrier of 1,3-butadiene and for the conrotatory ring opening of cyclobutene to the *gauche*-1,3-butadiene conformer. The energies of the conformers and the reaction barriers are calculated at both variational and diffusional Monte Carlo levels providing a precise picture of the potential energy surface of 1,3-butadiene and supporting one of the two model profiles recently obtained by Raman spectroscopy [Boopalachandran *et al.*, J. Phys. Chem. A **115**, 8920 (2011)]. Considering the good scaling of QMC techniques with the system's size, our results also demonstrate how variational Monte Carlo calculations can be applied in the future to properly investigate the reaction pathways of large and correlated molecular systems. © *2012 American Institute of Physics*. [http://dx.doi.org/10.1063/1.4769791]

I. INTRODUCTION

The 1,3-butadiene molecule,[1–6] C_4H_6, is the smallest conjugated diene which is greatly used in industry for the fabrication of various types of elastic polymers. In this paper we describe the geometries and energetics of two intramolecular reactions of this molecule: the rotation of the dihedral angle, connecting the *s-trans* and the *s-cis* planar states, and the conrotatory ring opening of cyclobutene in 1,3-butadiene (Fig. 1).

The potential energy surface derived from the dihedral torsion angle has been deeply studied with various experimental techniques[2,7–13] and quantum chemical calculations.[6,12,14–29] Through a first accurate gas-phase Raman scattering investigation by Engeln, Consalvo, and Reuss in 1992[30] four stationary points were recognized in the potential outline. The first lower energy conformer was recognized to be the planar *s-trans*-1,3-butadiene, followed by a *gauche* conformer which was found to be more stable then the planar *s-cis* one. This result has been recently confirmed by the Raman gas-phase spectra investigation published by Boopalachandran *et al.* in 2011.[31] Assuming the equilibrium structure calculated with the coupled cluster (CC) method in Ref. 29, Boopalachandran *et al.* used two different models to fit their accurate experimental data. The two models, namely A and B, differ in the assignation of some spectroscopic bands to different excitations: the authors considered more correct the band assignation made for model A, and this was even confirmed by the good compatibility with the torsion potential obtained through the accurate CC calculations of Ref. 29. In particular the two experimental models predict quite different excitation energies between the *s-cis* and the more stable *gauche* conformer: 0.517 kcal/mol and 1.164 kcal/mol for models A and model B, respectively.

The experimental information about the second reaction pathway - the conrotatory ring opening of cyclobutene and its isomerization in 1,3-butadiene - is principally related to the activation barrier studied through UV spectrometric analysis at high temperatures.[32–34] The reaction energy difference between the cyclobutene and *s-trans*-1,3-butadiene was deduced indirectly through the thermochemistry of the conversion between bicyclobutane and 1,3-butadiene.[35] The reaction has been computationally investigated at different levels of theory through *ab initio* methods like Hartree-Fock (HF), Møller-Plesset (MP) perturbation theory, configuration interaction (CI),[36–41] and density functional theory (DFT)[38,40–45] although the only calculation reporting the complete reaction pathway through internal reaction coordinates has been reported in Ref. 41 by MP2 and DFT methods.

For both the reactions the comparison between the experimental results and the various computational methods illustrate the point that, to correctly describe the molecular properties, electron correlation has to be taken into account. Indeed, post Hartree-Fock methods like CI, CC, and MP show a better agreement with the experimental results in describing both the geometries and the energies involved,[20,22,27,29,41–43] with respect to DFT calculations, no matter if generalized gradient approximation (GGA) or hybrid functionals are used.[25,38,41–43,45]

An alternative to all these methods which has attracted great interest in the recent years is represented by the collection of the correlated quantum Monte Carlo (QMC)

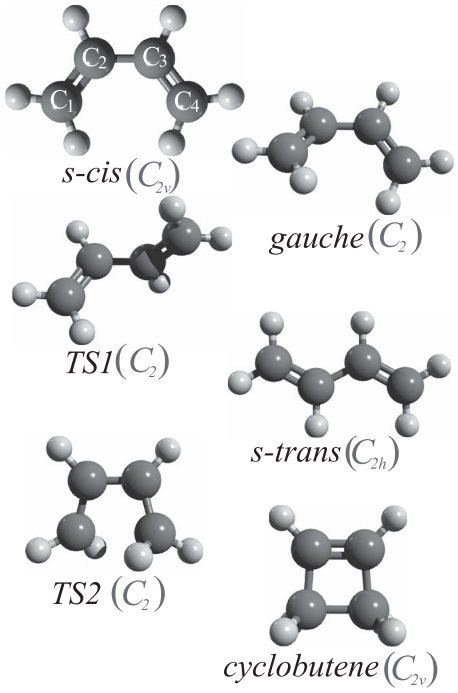

FIG. 1. Different 1,3-butadiene conformers and cyclobutene equilibrium state are shown. *TS1* refers to the transition state of the torsion barrier of 1,3-butadiene, while *TS2* refers to the ring opening barrier of cyclobutene. The geometrical symmetry of the conformers is reported in parenthesis.

methods, which have two computational advantages with respect to more traditional correlated quantum chemistry techniques. First, QMC has good scaling properties since the computational cost grows as $\mathcal{O}(N^{3-4})$ with the number N of electrons, at variance with $\mathcal{O}(N^{5-7})$. Second, the excellent parallelization of the algorithms makes these techniques extremely efficient on modern high performance computing (HPC) structures up to several tens of thousands of processors.[46] Even though for small systems QMC methods appear computationally unfavored, due to the overall time prefactor of these stochastic integration procedures, the two features described above are able to overcome the disadvantages of other high level quantum chemical methods for bigger systems. Up till now, also considering that the new computer facilities favor parallelization and small single processor memory allocations, QMC techniques are the only fully correlated *ab initio* methods which can be applied to large systems. Recent advancements in QMC force calculation, such as the one proposed by Sorella and Capriotti[47] have led to the possibility to perform the full geometry optimization of molecules with more then 50 atoms within the variational Monte Carlo (VMC) framework. This procedure has already been applied to the accurate calculation of equilibrium structures of several molecules, such as ethylene in singlet and triplet states,[48] the minimal retinal model[46,49] and its full protonated Schiff base within a quantum Monte Carlo / molecular mechanics framework.[50]

In the present paper we apply, for the first time to the best of our knowledge, QMC methods to evaluate directly the molecular geometries at the top of energy barriers with the aim to obtain a fully consistent potential energy curve along reaction coordinates, as well as an accurate estimation of the kinetic barriers and thermodynamics. This represents a step forward with respect to the common use of QMC in the study of reaction pathways, which is that of an accurate energy estimator on previously optimized geometries.[51–53] To optimize the molecular equilibrium structures, the Hessian matrix must be evaluated through energy or force calculations.[54] In a work by Wagner and Grossman in 2010,[55] the Hessian matrix was obtained at the diffusion Monte Carlo level for the H_2O-OH^- complex, through single energy calculations. In their work the wave function was optimized through DFT with PBE0 hybrid functional and with the addition of a three-body Jastrow factor.

In our work we present a more consistent approach through pure VMC calculations, that optimize both the molecular structure and all the wave function parameters simultaneously, with the stochastic evaluation of intramolecular forces.

For this reason we believe that the proposed investigation may open the way to the fully correlated characterization of transition states in chemical reactions involving large systems.

The paper is organized in the following way: in Sec. II we briefly describe the QMC methods used in our calculations, the wave function employed, the basis sets used and other computational details of our QMC calculations.

In Sec. III we discuss our results comparing them with the experimental results and high level quantum chemistry calculations. In Sec. IV we summarize these results giving prospectives on future implementations.

II. COMPUTATIONAL METHODS

A. Quantum Monte Carlo

VMC methods are based on the stochastic evaluation of the energy functional

$$E[\Psi_T(\{\bar{\alpha}, \bar{\mathbf{R}}\})] = \frac{\langle \Psi_T(\{\bar{\alpha}, \bar{\mathbf{R}}\})|\hat{H}|\Psi_T(\{\bar{\alpha}, \bar{\mathbf{R}}\})\rangle}{\langle \Psi_T(\{\bar{\alpha}, \bar{\mathbf{R}}\})|\Psi_T(\{\bar{\alpha}, \bar{\mathbf{R}}\})\rangle} \qquad (1)$$

with respect to a trial wave function $\Psi_T(\bar{\mathbf{x}}, \{\bar{\alpha}, \bar{\mathbf{R}}\}) = \langle \bar{\mathbf{x}}|\Psi_T(\{\bar{\alpha}, \bar{\mathbf{R}}\})\rangle$, where $\bar{\mathbf{x}}$ is the $6N$-dimensional vector of the electronic Cartesian and spin coordinates, $\bar{\alpha}$ is a set of independent wave function parameters, $\bar{\mathbf{R}}$ is the vector of the nuclear coordinates, and $\hat{\mathrm{H}}$ is the molecular Hamiltonian. The stochastic integration is done by rewriting the energy functional as the integral of the product of two multidimensional functions: the *local energy*, $E_L(\bar{\mathbf{x}}) = \langle \bar{\mathbf{x}}|\hat{H}|\Psi_T\rangle/\langle \bar{\mathbf{x}}|\Psi_T\rangle$, associated to a single electronic configuration $\bar{\mathbf{x}}$, and the probability $\Pi(\bar{\mathbf{x}}) = |\langle \bar{\mathbf{x}}|\Psi_T\rangle|^2/\langle \Psi_T|\Psi_T\rangle$ with which the configuration is generated. By sampling a certain number $\mathcal{N}$ of configurations, we can estimate the energy functional defined in Eq. (1) as the mean value of the local energies, $E[\Psi_T] \simeq E_{VMC} = [\sum_{i=1}^{\mathcal{N}} E_L(\bar{\mathbf{x}})]/\mathcal{N}$, with an error $\sqrt{(\langle E_L(\bar{\mathbf{x}})^2\rangle_{\mathcal{N}} - \langle E_L(\bar{\mathbf{x}})\rangle_{\mathcal{N}}^2)/\mathcal{N}}$ that decreases with the number $\mathcal{N}$ of sampled configurations. By minimizing Eq. (1) with respect to $\bar{\alpha}$ one can obtain an upper bound E_T of the ground state energy E_0 according to the variational principle. In our investigation the set of parameters $\bar{\alpha}$ are optimized using the linear method introduced in Ref. 56, that is based on the stochastic evaluation of the energy derivatives. In

the VMC scheme the structural optimization of molecules is done with a stochastic procedure recently introduced in Ref. 47, and already applied successfully in Refs. 46, 48, 54, and 57, providing an efficient and accurate evaluation of the atomic force vectors $\mathbf{F}_a(\bar{\mathbf{R}}) = -\nabla_{\mathbf{R}_a} E[\Psi_T(\bar{\mathbf{R}})]$ acting on all atomic positions $\bar{\mathbf{R}}$. The procedure is based on three computational features. The first one is the differential space warp coordinate transformation (SWCT) to calculate atomic forces within single VMC energy calculations[58–60] also treating non-local pseudopotentials. The second feature is the reweighting method introduced to solve the problem of infinite variance in the force calculations.[48,61] As previously described in Refs. 48 and 61 the expression of the force components can be written as the sum of two contributions

$$\begin{aligned}\mathbf{F}_a(\bar{\mathbf{R}}) = &-\left\langle \frac{dE_L(\bar{\mathbf{x}})}{d\mathbf{R}_a}\right\rangle_{\Pi(\bar{\mathbf{x}})} \\ &+2\left\{\langle E_L(\bar{\mathbf{x}})\rangle_{\Pi(\bar{\mathbf{x}})}\left\langle \frac{d\ln[\Psi_T(\bar{\mathbf{x}})]}{d\mathbf{R}_a}\right\rangle_{\Pi(\bar{\mathbf{x}})}\right. \\ &\left.-\left\langle E_L(\bar{\mathbf{x}})\frac{d\ln[\Psi_T(\bar{\mathbf{x}})]}{d\mathbf{R}_a}\right\rangle_{\Pi(\bar{\mathbf{x}})}\right\}, \end{aligned} \tag{2}$$

which are, respectively, the Hellmann-Feynman and the Pulay terms, both estimated as mean values $\langle\ldots\rangle_{\Pi(\bar{\mathbf{x}})}$ over the sampling probability $\Pi(\bar{\mathbf{x}})$. Both these terms suffer an infinite variance problem when an electronic configuration $\bar{\mathbf{x}}$ approaches the nodal surface. As the distance d between the electronic configuration and the nodal surface approaches to zero, the sampling probability goes as $\Pi(\bar{\mathbf{x}}) \simeq d^2$ while the derivative of the logarithm of the wave function diverges as $\simeq \frac{1}{d}$, and the derivative of the local energy that appears in the Hellmann-Feynman term diverges as $\simeq \frac{1}{d^2}$. These behaviors, that give well defined mean values, lead to undefined variances which are cured through the reweighting of the sampling probability $\Pi(\bar{\mathbf{x}})$, smoothly avoiding the overlap between the nodal surface and a configuration.

When using the SWCT in combination with pseudopotentials it is convenient to use an automated algorithm for the evaluation of the force components. The third computational feature is indeed the adjoint algorithmic differentiation,[47] which allows us to easily evaluate forces with a computational cost about four times the total cost of a single VMC energy calculation, independently on the number of the nuclei.

To verify the convergence and the quality of the VMC energy calculations, on the optimized wave functions and structural parameters, the lattice regularized diffusion Monte Carlo (LRDMC)[62,63] method is used. The LRDMC is a projection method based on the Green-function Monte Carlo method in a discretized space of grid spacing a. To overcome the error introduced by this discretization, the single point energy values are obtained by extrapolating the estimated energies for different a to the limit of continuum ($a \to 0$).

B. Variational wave function

The Jastrow antisymmetrised geminal power (JAGP)[64] wave function, derived from the resonating valence bond (RVB) picture introduced by Pauling,[65] is built as the product between an antisymmetric geminal power (AGP)[66] and a Jastrow factor $J(\bar{\mathbf{r}})$. This wave function, which is able to describe efficiently the static and dynamical electronic correlations, has already been successfully applied to the study of molecular ground and excited states,[48,67] on various types of chemical bonds like van der Waals interactions[56] or the hydrogen bond in the water dimer[68] and to calculate electronic state properties, like the dipole and quadrupole moments and polarizability.[69] In the case of closed shell molecular systems of N electrons in a spin singlet state, i.e., $N/2 = N^{\uparrow} = N^{\downarrow}$, the determinantal AGP part of the wave function is written as the antisymmetrized product:

$$\Psi_{AGP}(\bar{\mathbf{x}}) = \hat{A}\prod_{i=1}^{N/2}\Phi_G\left(\mathbf{x}_i^{\uparrow};\mathbf{x}_i^{\downarrow}\right) \tag{3}$$

of geminal functions

$$\Phi_G(\mathbf{x}_i;\mathbf{x}_j) = \sum_{a,b=1}^{M}\sum_{\mu,\nu}\lambda_{\mu_a\nu_b}\psi_{\mu_a}(\mathbf{r}_i)\,\psi_{\nu_b}\left(\mathbf{r}_j\right)|0,0\rangle \tag{4}$$

defined as a linear combination of products of two atomic orbitals, of quantum numbers μ, $\nu = (n, l, l_z)$ and centered on the ath and bth atoms, in a spin singlet state $|0, 0\rangle$. The Jastrow term is written as the product of three contributions, $J = J_1J_2J_{3/4}$, as described in Ref. 70. It includes homogeneous terms, that depend only on the relative distances, necessary to treat the nucleus-electron and electron-electron cusp conditions,[71] and non homogeneous terms that describe dynamical correlation effects.

C. Computational details

All the QMC calculations are carried out using the TURBORVB[72] package by Sorella and co-workers. To study the various conformers we have used two different, fully optimized basis sets, treating the core electrons of the carbon atoms with pseudopotentials. To test the effect of this substitution on our geometrical optimizations, two pseudopotentials are compared both including relativistic scalar correction: an energy-consistent (ECP)[73] and a norm-conserving pseudopotential (NCP).[74]

The two basis sets are defined through different contractions of the smaller Gaussian primitives of the cc-pVDZ basis set.[77] The bigger exponents are excluded because of the presence of the pseudopotential on the carbon atoms and on the fact that the hydrogen nuclear cusp is already described through the one-body Jastrow factor. Even though a good starting point for the total optimization of the wave function is generally welcome, when dealing with small molecules and small basis sets it is not a necessary requirement. On the other hand, the full optimization of the basis set, even when complete correlated consistent basis sets are used, is essential for the correct total energy minimization of the molecular compounds, and the optimization of the exponents usually lessens the energy of several tenths of hartree. The carbon atoms of the first basis set are described through two contracted s orbitals and two contracted p orbitals each built as the linear

combination of four Gaussian primitives (4s4p)/[2s2p]. The larger basis set for the carbon atoms consists of five Gaussian primitives for the *s* and *p* orbitals and two Gaussian primitives for the *d* orbitals, contracted in three *s* orbitals, two *p* and one *d* orbitals, i.e., (5s5p2d)/[3s2p1d]. The basis set for the hydrogen atoms is built by one contracted *s* orbital and one contracted *p*, both built as the linear combination of three Gaussian primitives (3s3p)/[1s1p]. The basis set used to build the one- and three-body Jastrow factors is fixed for the carbon atoms to four Gaussian primitives for *s* shells and three for the *p* shells, which are contracted in two *s* and *p* orbitals, i.e., (4s3p)/[2s2p]. The Jastrow basis set used for the hydrogen atoms is slightly smaller and consists in one contracted *s* orbital and one contracted *p* orbital, the first built as the combination of three Gaussian primitives, while the second built of two Gaussian primitives (3s2p)/[1s1p].

The use of these two relatively simple basis sets has been previously shown to be suitable for converged geometry optimizations for the ethylene molecule;[48] similar basis sets have been used for the Retinal minimal model.[46] In Secs. III and IV we will refer to these basis sets as VMC_1 and VMC_2, respectively. The wave function optimizations are done following the gradual steps described in Refs. 48 and 69, with the maximum number of 2×10^5 Monte Carlo (MC) steps per electron. The structural optimizations are done through 3000 variational steps with the same statistical accuracy used for the wave function optimizations, and the equilibrium geometries are obtained by averaging over the last 300 steps. VMC single point calculations are done with 6×10^7 MC steps per electron, while the LRDMC calculations are done extrapolating to the $a \rightarrow 0$ limit the energy calculations for different values of space discretization $a = \{0.1, 0.2, 0.3, 0.4\}$ a.u., each with an accuracy of 128×10^5 MC steps per electron. The parallelization of the Monte Carlo algorithms has been tested on BlueGene machines up to a maximum number of 65 000 processors, reporting nearly perfect scaling for VMC calculations and an efficiency loss of less then 3% for the geometry optimizations and the LRDMC calculations. Three thousand steps of full structural and wave function optimization for a single 1,3-butadiene conformer require 8 h on 2048 BG/P (850 MHz) cores with the biggest basis set. On the same basis set 500 wave function optimization steps require less then 2 h on the same number of cores. In a recent article, Guidoni and co-workers[46] have reported a table showing the computational cost of the QMC optimization procedures as a function of the number of valence electrons in the system.

III. RESULTS AND DISCUSSION

A. 1,3-butadiene torsion barrier

To study the torsion barrier of 1,3-butadiene the first step has been to optimize the wave functions and the structures of the *s-trans*, *s-cis*, and *gauche* conformers (Fig. 1).

While the *s-trans* and *s-cis* conformers are obtained by simply imposing, respectively, the C_{2h} and C_{2v} geometrical symmetries, the *gauche* stable conformer is obtained after the full relaxation of the *s-cis* conformer, permitting the torsion of the dihedral $\Delta_{C_1C_2C_3C_4}$ angle between the carbon atoms, so that the predicted C_2 symmetry is reached (Fig. 1).

To verify the convergence of the structures as a function of the basis sets, the structural optimizations are performed with the two different basis sets described in Subsection II C, and with both the NCP and ECP pseudopotentials, as reported in Table I. The reported errors are calculated along the final 300 consecutive structural configurations, taking into account the correction due to the correlation time.

Comparing the results for the two pseudopotentials several conclusions can be drawn. The first is that the geometrical optimizations with the NCP pseudopotential show a small elongation of about 0.005 Å of both the single and double bonds with respect to the ECP results, as previously shown in Ref. 48. As reported in the latter work for the case of ethylene, the geometrical parameters obtained through all-electron calculations give values of the bond lengths in between those obtained with the two pseudopotentials. These small differences cancel out in the evaluation of the bond length alternation (BLA) in the first column of Table I, for which it is clear that the bond differences are identical for both the ECP and NCP pseudopotentials. We also have to point out that within our QMC optimization scheme, also the smallest (VMC_1) basis set can provide us with converged structures in the statistical errors. Small geometrical differences can be observed in the bond angles.

Our *s-trans* results show a good agreement with the experimental structures. In line with different experimental results, the BLA of the *s-trans* conformer seems to be slightly larger than that obtained using other *ab initio* correlated computational methods like CCSD(T), MP2, and CASSCF (Table I). The result is independent on both the pseudopotential and the basis set used, and clearly demonstrates the capability of the QMC methods together with the JAGP wave function to well define the structural properties of conjugated systems. Although the differences between ECP and NCP are not large, to study the energetics of the reactions we preferred to use the ECP pseudopotential since, as previously shown by us,[48] its results are closer to all-electron calculations for what concerns excitation energies, even if it usually predicts slightly shorter bond lengths. Moreover, the ECP pseudopotential gives significantly smaller variances, 3−4 times smaller then those obtained with the NCP pseudopotential when calculating the single point energies of our molecular compounds.

To evaluate the energy and structure of the torsion barrier between the *s-trans* and the *gauche* conformers, we studied the potential energy surface along the reaction pathway defined by the torsion of the dihedral angle $\Delta_{C_1C_2C_3C_4}$, through geometrical optimizations performed by constraining $\Delta_{C_1C_2C_3C_4}$ at different values. The energy profile for VMC_1 is shown in Figure 2.

To obtain the geometrical structure of the *TS1* state, shown in Figure 1, a polynomial fit of the VMC_1 energies around the barrier was done, and the maximum was identified at an angle of about $77(1)^\circ$. By fixing the dihedral angle to this value, optimized geometries of the *TS1* conformer are obtained, as reported in Table II.

TABLE I. Equilibrium structures of 1,3-butadiene calculated by full VMC geometry optimizations are reported, together with other quantum chemistry calculations and experimental data. VMC_1 and VMC_2 stand for the calculations with the smaller and the larger basis sets, respectively, whereas (ECP) and (NCP) refer to the two pseudopotentials used to treat the core electrons of the carbon atoms, as described in Subsection II C.

	s-trans				*gauche*				*s-cis*		
	BLA (Å)	$R_{C_1C_2}$ (Å)	$R_{C_2C_3}$ (Å)	$\theta_{C_1C_2C_3}$ (deg)	$R_{C_1C_2}$ (Å)	$R_{C_2C_3}$ (Å)	$\theta_{C_1C_2C_3}$ (deg)	$\Delta_{C_1C_2C_3C_4}$ (deg)	$R_{C_1C_2}$ (Å)	$R_{C_2C_3}$ (Å)	$\theta_{C_1C_2C_3}$ (deg)
VMC_1(ECP)	0.1257(4)	1.3326(2)	1.4583(4)	123.66(2)	1.3313(2)	1.4694(3)	124.65(1)	143.09(2)	1.3323(1)	1.4726(2)	126.79(1)
VMC_2(ECP)	0.1252(2)	1.3328(1)	1.4580(2)	123.80(2)	1.3310(2)	1.4710(2)	125.26(1)	143.85(5)	1.3319(1)	1.4722(3)	126.57(1)
VMC_1(NCP)	0.1249(3)	1.3384(1)	1.4633(3)	123.65(2)					1.3389(2)	1.4767(5)	126.44(2)
VMC_2(NCP)	0.1258(4)	1.3387(2)	1.4645(4)	123.82(3)					1.3387(2)	1.4766(4)	126.63(2)
CASSCF[a]	0.118	1.345	1.463	124.1							
RASSCF[a]	0.117	1.351	1.468	123.9							
CASSCF[b]	0.128	1.344	1.467	124.0					1.345	1.476	126.9
CASPT2[b]	0.106	1.348	1.454	123.6					1.351	1.468	126.7
CCSD(T)[c]	0.1160	1.3389	1.4549	123.5	1.3362	1.4682	124.4	144.5	1.3371	1.4696	126.3
MP2[b]	0.113	1.343	1.456	123.7					1.342	1.470	126.5
MP2[d]	0.1132	1.3401	1.4533	123.54							
MP2[e]	0.1137	1.3425	1.4562	123.73	1.3415	1.4680	124.12	142.19			
B3LYP[b]	0.117	1.339	1.456	124.3					1.339	1.470	127.3
B3LYP[d]	0.1188	1.3339	1.4527	124.36							
B3LYP[f]	0.1183	1.3344	1.4527	124.35							
B3LYP[g]	0.12	1.34	1.46	124.27	1.34	1.47	125.87	147.19			
Semi-Exp[h]	0.1163(14)	1.3376(10)	1.4539(10)	123.62(10)							
SED[i]	0.1233(14)	1.3439(5)	1.4672(13)	122.8(5)							
ED[j]	0.122(3)	1.341(2)	1.463(3)	123.3(5)							
ED[k]	0.118(2)	1.349(1)	1.467(2)	124.4(1)							
MFTS[l]	0.130	1.337	1.467	123.5							
ED[m]	0.146	1.337	1.483	122.4							

[a]CASSCF(4,8)/6-31G*+3p and RASSCF(22,9+5+12)[1,1]/6-31G*+3p are taken from Ref. 26.
[b]Calculations with 6-31G(d) basis set from Ref. 24.
[c]CCSD(T)(FC)/CBS calculations from Ref. 29, that include core/valence (CV) and scalar relativistic (SR) corrections. For the geometry of the *s-trans* conformer also CCSDT(Q)(FC)/cc-pVDZ corrections are considered.
[d]Both calculations are made using the cc-pVTZ basis set, from Ref. 6.
[e]Calculations with 6-31G* basis set from Ref. 23.
[f]Calculations with auc-cc-pVTZ basis set from Ref. 28.
[g]Calculations from Ref. 25.
[h]Semi-experimental method from vibrational analysis described in Ref. 6.
[i]Sector electron diffraction from Ref. 4.
[j]Electron diffraction from Ref. 5.
[k]Electron diffraction from Ref. 75.
[l]Microwave Fourier transform spectrum from Ref. 76.
[m]Electron diffraction from Ref. 3.

In Figure 2 we compare our results for the torsional potential with the curves proposed by Ref. 31 on the basis of two different models (A and B) compatible with Raman scattering data.

The VMC results seem to confirm the value of the dihedral angle of the *TS1* transition state and of the *gauche* conformer in agreement with model A from Ref. 31. For the stable *gauche* conformer the geometrical relaxation of the *s-cis*-1,3-butadiene with both basis sets, gives an angle between 143.09(11)° and 143.86(17)° (Table I), while the models A and B from the Raman scattering results of Ref. 31 give angles of 142.89° and 131.05°, respectively.

In Table III we can see how the VMC_2 and LRDMC results for the activation barrier of this reaction, estimated by the difference between the *s-trans* and *TS1* energies, are comparable with the same (A) model proposed in Ref. 31 in the range between 6.31(31) and 6.68(11) kcal/mol.

The energy difference between the *s-trans* conformer and the *gauche* one seems to slightly depend on the basis set used. For the smallest basis set it is estimated to be of 2.69(16) and 2.72(30) kcal/mol from VMC and LRDMC calculations, respectively, while for the bigger basis set we obtain 3.28(11) and 3.14(29) kcal/mol from VMC and LRDMC calculations. The more accurate LRDMC results confirm the energy differences found for the *gauche* conformer in the model (A) of the recent Raman scattering experiments. For the *s-cis* conformer, we have a good agreement with the previous experimental model on the VMC level of theory, while the LRDMC predictions with both basis sets give higher energies (Table III) in the range between 3.84(30) and 3.94(29) kcal/mol, comparable with the Raman scattering results of Engeln, Consalvo, and Reuss.[30]

Comparing our results with those obtained by other post Hartree-Fock calculations reported in Tables II and III we can see that a good agreement with other correlated quantum chemical methods like CCSD(T)[27,29] and MP2[22,27] is found for both the structures of the *TS1* conformer and the energy differences. The VMC_1 activation barrier shown in Figure 2

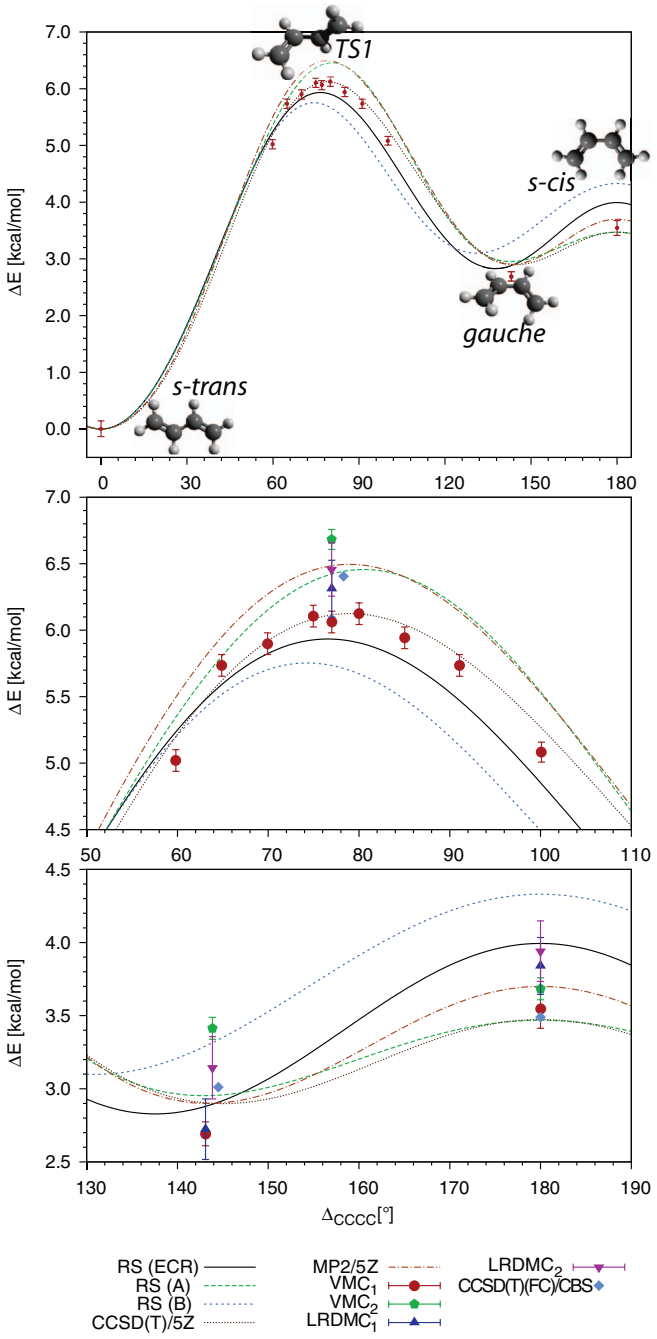

FIG. 2. Torsional potential of 1,3-butadiene in the upper panel. In the centre panel the torsional potential around the activation barrier is reported. In the bottom panel the energy difference between the *gauche* and *s-cis* conformers is shown. RS (ECR) is the Raman spectra from Ref. 30; RS (A) and (B) are the two distinct models from Ref. 31; CCSD(T)/5Z and MP2/5Z are the curves obtained with cc-pV5Z basis set from Ref. 27; CCSD(T)(FC)/CBS with core/valence, scalar-relativistic and CCSDT(Q)/cc-pVDZ corrections are from Ref. 29. VMC_1 and $LRDMC_1$, VMC_2 and $LRDMC_2$ are the variational and lattice regularized diffusion Monte Carlo results referring to the two basis sets described in Subsection II C. Some values are listed in Table III.

has a nearly perfect agreement with the CCSD(T)/cc-pV5Z[27] curve, while a small discrepancy of less than 0.5 kcal/mol can be identified with the CCSD(T)(FC)/CBS calculations with Q corrections form Ref. 29. When LRDMC is used, the obtained values are fully compatible with both the corrected CCSD(T)(FC)/CBS[29] and MP2/cc-pV5Z[27] results.

TABLE II. VMC estimated geometry of the transition state between the *s-cis* and *s-trans* torsional barrier *TS1*. The VMC results are calculated using the ECP pseudopotential to substitute the core electrons of the carbon atoms. The dihedral angle $\Delta_{C_1C_2C_3C_4}$ is fixed through an harmonic constraint.

	$R_{C_1C_2}$ (Å)	$R_{C_2C_3}$ (Å)	$\theta_{C_1C_2C_3}$ (deg)	$\Delta_{C_1C_2C_3C_4}$ (deg)
VMC_1	1.3282(4)	1.4843(7)	124.26(1)	76.999(8)
VMC_2	1.3282(1)	1.4844(2)	124.23(1)	76.988(4)
CCSD(T)[a]	1.3327	1.4824	123.8	78.3
MP2[b]	1.341	1.486	123.4	77.9
MP2[c]	1.340	1.483	123.6	78.4
BLYP[c]	1.345	1.496	124.8	80.0

[a]CCSD(T)(FC)/CBS calculations with core/valence (CV) and scalar-relativistic (SR) corrections from Ref. 29.
[b]MP2 6-311G** calculations from Ref. 21.
[c]Calculations with 6-31G* from Ref. 38.

In summary, our QMC results confirm the (A) model from the Raman scattering results of Ref. 31 with a small difference in the energy of the *s-cis* conformer, predicted to be 0.5 kcal/mol higher in energy by our LRDMC results.

TABLE III. Energy gaps of 1,3-butadiene conformers calculated with respect to the *s-trans* conformer are reported, without considering zero point energy corrections, and referring to the PES reported in Figure 2. The QMC calculations are done on the geometries reported in Tables I and II, with ECP pseudopotential.

	TS1 (kcal/mol)	*gauche* (kcal/mol)	*s-cis* (kcal/mol)
VMC_1	6.06(17)	2.69(16)	3.54(19)
VMC_2	6.68(11)	3.28(11)	3.68(11)
$LRDMC_1$	6.31(31)	2.72(30)	3.84(30)
$LRDMC_2$	6.46(28)	3.14(29)	3.94(29)
HF[a]	6.23	3.51	4.34
CCSD(T)[b]	6.124	2.899	3.474
CCSD(T)[c]	6.405	3.011	3.489
CCSD(T)[a]	6.06	3.05	3.43
G2[d]	5.67	2.92	3.45
CBS-Q[d]	6.02	3.16	3.38
MP2[b]	6.496	2.899	3.697
MP2[a]	6.53	3.02	3.65
B3LYP[e]	7.54	3.97	
UV[f]		3.02(1)	
RS (ECR)[g]	5.93	2.85	4.00
GF-RS (A)[h]	6.456	2.951	3.468
GF-RS (B)[h]	5.684	3.091	4.254

[a]HF calculations are done with a cc-pVQZ basis while MP2 results are extrapolated and CCSD(T) results are obtained with a cc-pVDZ basis set. Reference 22.
[b]Both calculations done with cc-pV5Z basis set from Ref. 27.
[c]CCSD(T)(FC)/CBS with core/valence, scalar relativistic and CCSDT(Q)(FC)/cc-pVDZ corrections from Ref. 29.
[d]G2 is based on QCISD(T)/6-311+G(3df,2p) calculations on an MP2/6-31G* evaluated geometry, CBS-Q is based on MP2/6-311++G(3df,2p) calculations with higher order corrections from MP4(SDQ)/6-31+G(2d,p) and QCISD(T)/6-31+G on MP2/6-31G* geometries, both from Ref. 20.
[e]Calculations with TZVP basis from Ref. 25.
[f]The value of 2.93(1) reported in Ref. 78 is the ΔH° value obtained through UV spectra. To this value we have added the zero point energy difference between the *gauge* and *s-trans* state obtained in Ref. 29 through CCSD(T)(FC) calculations (+0.09 kcal/mol).
[g]Raman Spectra from Ref. 30.
[h]Gas Phase Raman Spectra (25°-200°) from Ref. 31.

TABLE IV. VMC equilibrium structures of cyclobutene calculated for both basis sets with the ECP pseudopotential, compared with other quantum chemistry calculations and experimental results from microwave spectra.

	$R_{C_2C_3}$ (Å)	$R_{C_1C_2}$ (Å)	$R_{C_1C_4}$ (Å)	$\theta_{C_1C_2C_3}$ (deg)
VMC_1	1.3352(2)	1.5135(2)	1.5642(3)	94.339(6)
VMC_2	1.3343(2)	1.5135(2)	1.5625(5)	94.324(10)
HF[a]	1.323	1.515	1.562	94.5
MP2[b]	1.350	1.519	1.569	94.1
MP2[a]	1.347	1.513	1.564	94.1
LDA[b]	1.338	1.502	1.554	94.2
NL-SCF[b]	1.346	1.525	1.579	94.3
ACM[a]	1.340	1.513	1.565	94.3
BLYP[a]	1.352	1.529	1.586	94.4
B3LYP[c]	1.339	1.519	1.573	94.4
MW[d]	1.342(4)	1.517(3)	1.566(3)	94.2

[a]Calculations with 6-31G* from Ref. 38.
[b]MP2 calculations were done with 6-311G** basis sets, while the LDA and NL-SCF calculations were done using the TZ+2P basis set; from Ref. 41.
[c]With basis set 6-311++G** from Ref. 43.
[d]Microwave spectra from Ref. 79.

B. Conrotatory ring opening of cyclobutene

The study of the reaction pathway for the isomerization process of cyclobutene requires the knowledge and the definition of a complex collective internal reaction coordinate.[41]

For the purpose of this work, we have chosen a simplified, albeit not perfect, reaction coordinate simply using the distance between the C_1 and C_4 carbon atoms. A better definition of the reaction coordinate and of the reaction path would require the adaptation of transition state search algorithms to error affected energy surfaces, requiring additional investigations that will be addressed in further studies.

First we optimized the structure of the stable cyclobutene (Fig. 1) molecule for both the VMC_1 and VMC_2 basis sets, as reported in Table IV. To the best of our knowledge the only experimental values for the structural parameters of cyclobutene have been obtained from microwave spectra analysis.[79] Our VMC calculations (Table IV) predict carbon bonds usually 0.005 Å shorter then the experimental ones. This could be due to the effect of the pseudopotential used for the carbon atoms as discussed above and as shown for the other stable conformers. After optimizing the structures of the cyclobutene molecule, the ring opening barrier was investigated by varying the $C_1\cdots C_4$ bond, relaxing at each distance all the other atomic positions, and calculating the corresponding variational energies.

In this way we were able to identify with accuracy the length of this bond near the potential barrier, as reported in Table V, which was found to be equal to 2.1389(2) Å. A small change of 2×10^{-4} Å in the $C_1\cdots C_4$ is enough to induce a drastic change of other structural parameters, for example the dihedral angle varies from 3° to 26° when crossing the *TS2* barrier between cyclobutene and the *gauche* conformer. This sharp transition is due to the presence of a conical intersection at its peak[80] and in a not optimal choice of the reaction coordinate.[41]

TABLE V. Energy gaps along the ring opening reaction of cyclobutene calculated with respect to the cyclobutene ground state energies. In the last column we reported the estimated $C_1\cdots C_4$ bond distance at the top of the *TS2* cyclization barrier. All QMC calculations are done with the ECP pseudopotential to replace the core electrons of the carbon atoms.

	s-trans (kcal/mol)	*gauche* (kcal/mol)	*TS2* (kcal/mol)	$R_{C_1C_4}$ (Å)
VMC_1	−11.83(16)	−9.14(11)	36.25(11)	2.1389(2)
VMC_2	−11.93(11)	−8.65(11)	36.51(10)	
$LRDMC_1$	−11.83(31)	−9.11(30)	35.34(31)	
$LRDMC_2$	−12.22(28)	−9.07(29)	35.23(29)	
HF[a]		−13.05	49.26	2.130[b]
MP2[c]	−8.1	−5.5	35.3	2.131
MP4[c]	−9.8	−7.2	35.3	
QCISD(T)[d]		−8.47	34.42	
B3LYP[e]		−12.82	31.59	2.137
B3LYP[d]		−12.15	31.62	2.138
B3LYP[a]		−12.55	36.46	
BLYP[f]	−14.03	−10.25	31.41	2.142
NL-P[c]	−13.5	−9.3	30.9	2.148
NL-SCF[c]	−13.2	−9.3	31.3	
Exp[34]			34.5(7)[g]	
Exp[33]			34.3(8)[g]	
Exp[32]			34.1(5)[g]	
Exp[35]	−10.54[h]			

[a]Energies from Ref. 42 with basis set 6-311G**.
[b]Structure obtained with 6-31G* from Ref. 38.
[c]The MP energies are obtained on MP2/6-311G** geometries, while the DFT calculations refer to a NL-SCF/TZ+2P geometrical optimization from Ref. 41.
[d]Both results obtained on B3LYP optimized geometries with 6-311++G** basis sets from Ref. 43.
[e]Calculations with 6-311+G(d,p) basis set from Ref. 45.
[f]Calculations with 6-31G* basis set from Ref. 38.
[g]To compare these results with the quantum chemical calculations presented we have removed the ZPE contributions estimated with the QCISD(T) method and reported in Ref. 43, which are equivalent to +1.6 kcal/mol. The published experimental values are 32.9(7),[34] 32.7(8)[33] and 32.5(5).[32]
[h]From the published experimental value of −11.5[35] we have removed the ZPE contributions estimated through the HF calculations of Ref. 38, and equal to +0.96 kcal/mol.

Despite this drawback, we can still give a rather accurate estimation of the activation energy for the ring opening process, i.e., the energy difference between the cyclobutene and the *TS2* transition state. Both the activation energy and the reaction energy are reported for the VMC and LRDMC calculations in Table V without zero point energy (ZPE) corrections. In Table V we also report the difference between the energy of the cyclobutene and the *gauche*-1,3-butadiene. For the activation energy the LRDMC results give a value nearly 1 kcal/mol lower then the VMC calculations in the range between 35.34(31) and 35.23(29) kcal/mol. To compare the calculations with the experimental values,[32–34] in the latter we have removed the ZPE contributions estimated with the QCISD(T) method and reported in Ref. 43, which are equivalent to +1.6 kcal/mol. The experimental results, that have been corrected in this way, appear to be still 1 kcal/mol lower in energy when compared to our LRDMC calculations, in the range between 34.1(5) and 34.5(7)[32–34] kcal/mol. The MP2 and MP4 results from Ref. 41 give values for the activation energy of the reaction that are comparable with our results, while the highest level of theory QCISD(T) predictions of Ref. 43 are practically coincident with the experimental

analysis. The DFT calculations seem to give values highly dependent on the basis sets, sometimes overestimating[42] and usually underestimating[38,41,43,45] the barrier by 2–3 kcal/mol.

The values of the reaction energy that have been obtained with both the VMC and LRDMC methods are all in the interval between −11.83(16) and −12.22(28) kcal/mol. These values should be compared with the experimental result of −10.46 kcal/mol[35] corrected by +0.96 kcal/mol due to the removing of the ZPE contributions estimated in Ref. 38 through HF calculations. Our QMC calculations appear to estimate a reaction energy which is 1 kcal/mol lower than the experimental value, while the MP4 calculations, which give results of the same order, appear to predict an energy gap that is 1 kcal/mol higher, and unfortunately no QCISD(T) calculations were reported. Similarly to the discrepancies observed for the activation energy, the DFT reaction energy is about 3 kcal/mol lower than the experimental value, quite distant from the estimations made through the *ab initio* methods. By looking at the last energy difference (Table V), between cyclobutene and the *gauche*-1,3-butadiene molecule we can see that our VMC and LRDMC results, between −8.65(11) and −9.11(29) kcal/mol are comparable with the QCISD(T)[43] value, lower then MP4[41] of about 2 kcal/mol.

In conclusion these results although problematic for the choice of an improper reaction coordinate, show that the QMC results are extremely reliable even in those cases in which great chemical accuracy is needed.

IV. CONCLUSIONS

In this work we have presented, for the first time, the study of chemical reactions using a full quantum Monte Carlo geometry relaxation along reaction coordinates. The great advantages of this correlated method, as for instance implemented in the TURBORVB[72] package, are its favorable scaling properties, $\mathcal{O}(N^{3-4})$ of the number N of electrons.

We have considered two pathways of the 1,3-butadiene chemistry: the *s-cis*/*s-trans* isomerization, and the conrotatory cyclization. The estimated *s-cis* to *s-trans* activation energy and the corresponding transition state geometry are in good agreement with other high level quantum chemistry calculations. VMC calculations predict an activation barrier in the range of 6.06(17)–6.68(11) kcal/mol, similarly to LRDMC results (6.31(31)–6.46(28) kcal/mol). The calculated energy profile along the torsional reaction path is compared with data from Raman scattering experiments supporting a recent analysis of Raman data (model A in Ref. 31). For the conrotatory cyclization we have estimated at LRDMC level the cyclobutene ring opening activation energy in the range between 35.34(31) and 35.23(29), in fair agreement with the experimental results within 1 kcal/mol. A similar discrepancy has been found for the calculation of reaction energies.

In conclusion, we have demonstrated the possibility to obtained through the VMC method accurate transition state geometries for the torsion barrier of 1,3-butadiene, and also accurate energy differences within both the VMC and LRDMC levels of theory. As the LRDMC results depend only on the nodal surface of the wave function, the energy differences calculated with this method over wave functions optimized at the VMC level are to be considered more accurate and in fact show in the case of the ring opening of cyclobutene a greater compatibility with the experimental values. These results demonstrate how QMC methods are able to provide accurate transition state geometries and energies even at the variational level, opening interesting perspectives to the study at high-correlation level of chemical reactions involving large molecules.

ACKNOWLEDGMENTS

The authors thank Professor Sandro Sorella for the development of the TURBORVB quantum Monte Carlo code, and Dr. Emanuele Coccia for the implementation of harmonic constraints in the code and for the accurate revision of this article. The authors acknowledge funding provided by the European Research Council (Project No. 240624) within the VII Framework Program of the European Union. For the availability of high performance computing resources and support we acknowledge the CINECA Award *IscrB_QMC-BLA-2011*, the PRACE Tier-0 Project PRA053, and the *Caliban* HPC center of the University of L'Aquila.

[1] R. B. Scott, R. D. Rands, Jr., C. H. Meyers, F. G. Brickwedde, and N. Bekkedahl, J. Res. Natl. Bur. Stand. **35**, 39 (1945).
[2] J. G. Aston, G. Szasz, H. W. Woolley, and F. G. Brickwedde, J. Chem. Phys. **14**, 67 (1946).
[3] A. Almenningen, O. Bastiansen, and M. Traetteberg, Acta Chem. Scand. **12**, 1221 (1958).
[4] W. Haugen and M. Traetteberg, Acta Chem. Scand. **20**, 1726 (1966).
[5] K. Kuchisu, T. Fukuyama, and Y. Morino, J. Mol. Struct. **1**, 463 (1968).
[6] N. C. Craig, P. Groner, and D. C. McKean, J. Phys. Chem. A **110**, 7461 (2006).
[7] M. E. Squillacote, R. S. Sheridan, O. L. Chapman, and F. A. L. Anet, J. Am. Chem. Soc. **101**, 3657 (1979).
[8] J. J. Fisher and J. Michl, J. Am. Chem. Soc. **109**, 1056 (1987).
[9] B. R. Arnold, V. Balaji, and J. Michl, J. Am. Chem. Soc. **112**, 1808 (1990).
[10] B. R. Arnold, V. Balaji, J. W. Downing, J. G. Radziszewski, J. J. Fisher, and J. Michl, J. Am. Chem. Soc. **113**, 2910 (1991).
[11] C. H. Choi, M. Kertesz, S. Dobrin, and J. Michl, Theor. Chem. Acc. **102**, 196 (1999).
[12] K. B. Wiberg and R. E. Rosenberg, J. Am. Chem. Soc. **112**, 1509 (1990).
[13] R. L. Lipnick and E. W. Garbisch, J. Am. Chem. Soc. **95**, 6370 (1973).
[14] L. Radom and J. A. Pople, J. Am. Chem. Soc. **92**, 4786 (1970).
[15] U. Pincelli, B. Cadioli, and B. Lévy, Chem. Phys. Lett. **13**, 249 (1972).
[16] P. Skancke and J. E. Boggs, J. Mol. Struct. **16**, 179 (1973).
[17] B. Dumbacher, Theor. Chem. Acc. **23**, 346 (1972).
[18] S. Skaarup, J. Boggs, and P. Skancke, Tetrahedron **32**, 1179 (1976).
[19] C. W. Bock, P. George, and M. Trachtman, Theor. Chem. Acc. **64**, 293 (1984).
[20] M. A. Murcko, H. Castejon, and K. B. Wiberg, J. Phys. Chem. **100**, 16162 (1996).
[21] X. Gong and H. Xiao, Int. J. Quantum Chem. **69**, 659 (1998).
[22] J. C. Sancho-García, A. J. Pérez-Jiménez, J. M. Pérez-Jordá, and F. Moscardó, Mol. Phys. **99**, 47 (2001).
[23] Y. N. Panchenko, J. V. Auwera, Y. Moussaoui, and G. R. De Maré, Struct. Chem. **14**, 337 (2003).
[24] C. S. Page and M. Olivucci, J. Comput. Chem. **24**, 298 (2003).
[25] S. Saha, F. Wang, C. T. Falzon, and M. J. Brunger, J. Chem. Phys. **123**, 124315 (2005).
[26] M. Boggio-Pasqua, M. J. Bearpark, M. Klene, and M. A. Robb, J. Chem. Phys. **120**, 7849 (2004).
[27] A. Karpfen and V. Parasuk, Mol. Phys. **102**, 819 (2004).
[28] D. C. McKean, N. C. Craig, and Y. N. Panchenko, J. Phys. Chem. A **110**, 8044 (2006).
[29] D. Feller and N. C. Craig, J. Phys. Chem. A **113**, 1601 (2009).
[30] R. Engeln, D. Consalvo, and J. Reuss, Chem. Phys. **160**, 427 (1992).

[31]P. Boopalachandran, N. Craig, P. Groner, and J. Laane, J. Phys. Chem. A **115**, 8920 (2011).
[32]W. Cooper and W. D. Walters, J. Am. Chem. Soc. **80**, 4220 (1958).
[33]W. P. Hauser and W. D. Walters, J. Phys. Chem. **67**, 1328 (1963).
[34]R. W. Carr and W. D. Walters, J. Phys. Chem. **69**, 1073 (1965).
[35]K. B. Wiberg and R. A. Fenoglio, J. Am. Chem. Soc. **90**, 3395 (1968).
[36]D. C. Spellmeyer and K. N. Houk, J. Am. Chem. Soc. **110**, 3412 (1988).
[37]M. A. McAllister and T. T. Tidwell, J. Am. Chem. Soc. **116**, 7233 (1994).
[38]J. Baker, M. Muir, and J. Andzelm, J. Chem. Phys. **102**, 2063 (1995).
[39]P. Celani, F. Bernardi, M. Olivucci, and M. A. Robb, J. Chem. Phys. **102**, 5733 (1995).
[40]O. Wiest, D. C. Montiel, and K. N. Houk, J. Phys. Chem. A **101**, 8378 (1997).
[41]L. Deng and T. Ziegler, J. Phys. Chem. **99**, 612 (1995).
[42]P. K. Chattaraj, P. Fuentealba, B. Gómez, and R. Contreras, J. Am. Chem. Soc. **122**, 348 (2000).
[43]P. Deng, L.-C. Li, A.-M. Tian, and N.-B. Wong, Int. J. Quantum Chem. **100**, 288 (2004).
[44]L. Guidoni and U. Rothlisberger, J. Chem. Theory Comput. **1**, 554 (2005).
[45]M. Jaccob, I. Sheeba Jem, S. Giri, P. Venuvanalingam, and P. K. Chattaraj, J. Phys. Org. Chem. **24**, 460 (2011).
[46]E. Coccia and L. Guidoni, J. Comput. Chem. **33**, 2332 (2012).
[47]S. Sorella and S. Capriotti, J. Chem. Phys. **133**, 234111 (2010).
[48]M. Barborini, S. Sorella, and L. Guidoni, J. Chem. Theory Comput. **8**, 1260 (2012).
[49]O. Valsson, C. Angeli, and C. Filippi, Phys. Chem. Chem. Phys. **14**, 11015 (2012).
[50]E. Coccia, D. Varsano, and L. Guidoni, "Protein field effect on the dark state of 11-*cis* retinal in rhodopsin by quantum Monte Carlo/molecular mechanics," J. Chem. Theory Comput. (published online).
[51]J. C. Grossman, W. A. Lester, and S. G. Louie, J. Am. Chem. Soc. **122**, 705 (2000).
[52]C. Filippi, S. B. Healy, P. Kratzer, E. Pehlke, and M. Scheffler, Phys. Rev. Lett. **89**, 166102 (2002).
[53]A. C. Kollias, O. Couronne, and J. W. A. Lester, J. Chem. Phys. **121**, 1357 (2004).
[54]A. Zen, D. Zhelyazov, and L. Guidoni, J. Chem. Theory Comput. **8**, 4204 (2012).
[55]L. K. Wagner and J. C. Grossman, Phys. Rev. Lett. **104**, 210201 (2010).
[56]S. Sorella, M. Casula, and D. Rocca, J. Chem. Phys. **127**, 14105 (2007).
[57]G. Mazzola, A. Zen, and S. Sorella, J. Chem. Phys. **137**, 134112 (2012).
[58]C. J. Umrigar, Int. J. Quantum Chem. **36**, 217 (1989).
[59]R. Assaraf and M. Caffarel, J. Chem. Phys. **119**, 10536 (2003).
[60]O. Valsson and C. Filippi, J. Chem. Theory Comput. **6**, 1275 (2010).
[61]C. Attaccalite and S. Sorella, Phys. Rev. Lett. **100**, 114501 (2008).
[62]M. Casula, C. Filippi, and S. Sorella, Phys. Rev. Lett. **95**, 100201 (2005).
[63]M. Casula, S. Moroni, S. Sorella, and C. Filippi, J. Chem. Phys. **135**, 154113 (2010).
[64]M. Casula and S. Sorella, J. Chem. Phys. **119**, 6500 (2003).
[65]L. Pauling, *The Nature of the Chemical Bond*, 3rd ed. (Cornell University Press, Itaca, New York, 1960), pp. 230–240.
[66]J. A. Pople, Proc. R. Soc. London, Ser. A **202**, 323 (1950).
[67]M. Casula, M. Marchi, S. Azadi, and S. Sorella, Chem. Phys. Lett. **477**, 255 (2009).
[68]F. Sterpone, L. Spanu, L. Ferraro, S. Sorella, and L. Guidoni, J. Chem. Theory Comput. **4**, 1428 (2008).
[69]E. Coccia, O. Chernomor, M. Barborini, S. Sorella, and L. Guidoni, J. Chem. Theory Comput. **8**, 1952 (2012).
[70]M. Marchi, S. Azadi, C. Casula, and S. Sorella, J. Chem. Phys. **131**, 154116 (2009).
[71]N. D. Drummond, M. D. Towler, and R. J. Needs, Phys. Rev. B **70**, 235119 (2004).
[72]S. Sorella, TURBORVB quantum Monte Carlo package, see http://people.sissa.it/~sorella/web/index.html.
[73]M. Burkatzki, C. Filippi, and M. Dolg, J. Chem. Phys. **126**, 234105 (2007).
[74]J. R. Trail and R. J. Needs, J. Chem. Phys. **122**, 174109 (2005).
[75]K. Kveseth, R. Seip, and D. A. Kohl, Acta Chem. Scand., Ser. A **34**, 31 (1980).
[76]W. Caminati, G. Grassi, and A. Bauder, Chem. Phys. Lett. **148**, 13 (1988).
[77]T. H. Dunning, J. Chem. Phys. **90**, 1007 (1989).
[78]J. Saltiel, D. F. Sears, and A. M. Turek, J. Phys. Chem. A **105**, 7569 (2001).
[79]B. Bak, J. Led, L. Nygaard, J. Rastrup-Andersen, and G. Sørensen, J. Mol. Struct. **3**, 369 (1969).
[80]M. Olivucci, I. N. Ragazos, F. Bernardi, and M. A. Robb, J. Am. Chem. Soc. **115**, 3710 (1993).